Are RAFT and ATRP Universally Interchangeable Polymerization Methods in Network Formation?

Julia Cuthbert[‡,a], *Shiwanka V. Wanasinghe*[‡b], *Krzysztof Matyjaszewski*[*,a], *Dominik Konkolewicz*[*,b]

[a] Department of Chemistry, Carnegie Mellon University, 4400 Fifth Ave, Pittsburgh, PA, 15213 USA

[b] Department of Chemistry and Biochemistry, Miami University, 651 E High St Oxford, OH, 45056, USA

‡ Co-first authors

* Corresponding authors: KM: matyjaszewski@cmu.edu, DK: d.konkolewicz@miamiOH.edu

Keywords

RDRP; ATRP; RAFT polymerization; gels; networks; polymer architecture

Abstract

Polymer networks were synthesized by both ATRP and RAFT to evaluate whether the choice of reversible deactivation radical polymerization method impacted the materials characteristics at either the molecular or bulk property level. Since control in ATRP is gained through interactions of a small molecule catalyst with the polymer chain end, rather than degenerative transfer between two polymer chain ends, ATRP could lead to better controlled networks, particularly after gelation. In general, both RAFT and ATRP gave better controlled materials than the corresponding FRP processes. In general RAFT reached higher conversions with higher gel fractions. The molecular properties indicate relatively small differences in control over primary polymer chain length and

dispersity of the primary chains at lower targeted chain lengths of 100 or 200 units. However, ATRP provided better controlled polymers at longer primary chains lengths of 500 units. Both RAFT and ATRP networks swelled to greater extents than their conventional radical analogues, with ATRP giving somewhat higher swelling ratios at longer primary chain lengths and lower crosslink densities. Rheological analysis indicates that both materials are similar, although RAFT gave materials with higher elastic moduli, consistent with the higher conversion and lower sol fraction in RAFT. Overall, both RAFT and ATRP formed materials with similar properties at lower chain lengths, with ATRP appearing to yield slightly better properties at longer chain lengths. The control in RAFT and ATRP is likely through soluble components, including the small molecule catalyst in ATRP and soluble polymer fractions (sol) in RAFT.

Introduction

Polymer gels and networks are crosslinked, three-dimensional materials that reversible absorb solvent and maintain their shape. Significant effort has been devoted to understanding gelation processes and the architecture at the macromolecular, nano and macroscopic scale.[1-4] Indeed, network structure is intimately tied to the material properties,[5-7] therefore it is critical to understand the impact of synthetic methods on network architecture and final material properties.[8] Eighty years ago, the first theory of gelation was proposed by Flory and Stockmayer.[9-12] Recently, theoretical improvements have been developed beyond the Stockmayer/Flory approach.[13] However, these theories included two idealized assumptions. The first is equal reactivity of monomers and crosslinkers. Additionally, the theory assumed a homogenous, perfect network structure with no defects, such as intermolecular cyclization or dangling chains.[14] Further investigations have focused on developing a cohesive theory which accounts for synthetic parameters, such as solvent effects, method of polymerization, or network defects.[8] In particular, the choice of a synthetic technique could have a substantial impact on the 3D network structure, whether step-growth polymerization, chain-growth polymerization, click-linking reactions, etc.[8] For example, a semi-batch monomer addition method was effective at decreasing the number of loop defects during network formation.[15] Another method to avoid topological defects is coupling the chain ends of pre-synthesized well-defined star polymers.[16,17]

The aim of this article is to compare the networks made by two reversible deactivation radical polymerization (RDRP) methods: atom transfer radical polymerization (ATRP)[18-20] and reversible addition-fragmentation chain transfer (RAFT) polymerization.[21,22] In general, RDRP networks are more regular and swell more than networks prepared by conventional free radical polymerization (FRP) processes dominated by chain breaking reactions.[14,23] This was first demonstrated by the delayed gel points and higher swelling of polystyrenes crosslinked with divinyl benzene prepared by nitroxide mediated polymerization, as compared to those formed by FRP.[2,24,25] Moreover, it has been reported that either ATRP or RAFT gels are more uniform and homogenous than their FRP analogues.[1,14,26-28] In an FRP process, radicals are generated, propagate, and then terminate, with the entire chain growth occurring within ~1 s. Early in the polymerization, dense nanogels are formed which are crosslinked later during the reaction to form a heterogeneous network. In both ATRP and RAFT methods, the growing polymer chain ends are reversibly and intermittently activated to alternate between active growing radicals and dormant chain ends. Consequently, it is possible to control the molecular weight, degree of polymerization (DP), dispersity (Đ), and to reinitiate the dormant chains to add further polymer block(s).[29-33] Due to the reversible activation/deactivation, linear chains are formed in the early stages of gelation instead of nanoclusters. As more crosslinkers are incorporated, the chains continue to branch, forming high molecular weight fractions (sol), and finally a network at the gel point.[1] After the gel point, fraction of sol decreases and progressively more gel is formed.

The main question for this study is how equivalent or different are networks prepared by ATRP and RAFT polymerizations. Although reversible deactivation and controlled/living polymerization networks have been demonstrated to have improved uniformity compared to conventional FRP, there is no detailed comparison of the nature of the various RDRP processes on the network properties. There has been work to understanding the different gelation kinetics between ATRP, RAFT, and conventional FRP, but there was no further characterization performed on the final materials.[26] In addition, two groups have reported that ATRP synthesized thermally responsive hydrogels have slower deswelling kinetics than the FRP hydrogels.[34-36] However, similar research comparing RAFT and FRP made thermally responsive hydrogels found that the FRP hydrogels exhibited a significantly slower deswelling rate.[37]

Although both ATRP and RAFT operate on the principle of reversible activation/deactivation, there are substantial mechanistic differences between the methods. In ATRP, an atom (usually a halogen, such as bromine (Br)) is reversibly transferred between the active and dormant polymer chain ends via a small molecule catalyst (commonly a copper/ligand complex). In RAFT polymerization, the radical degeneratively transfers or "shuttles" between chain ends, changing between an active radical and dormant thiocarbonylthio chain transfer agent (CTA) capped chain (Figure 1A and B). This requires direct contact between polymer chain ends which could be hampered in highly viscous media (especially in crosslinked gels and networks with immobilized chains). Thus, we hypothesized that, when synthesized under analogous conditions, the ATRP networks could be more homogeneous and primary chains should have Đ lower than the chains formed by RAFT. In both ATRP and RAFT, the polymerization parameters such as exchange rate coefficients are likely to be impacted by medium and viscosity effects as the system approaches gelation. However it is anticipated that the effects would be more significant for RAFT due to the bi-macromolecular nature of the activation/deactivation process. In this study RAFT and ATRP networks were synthesized, under conditions that are as similar as possible. To achieve this, thermally initiated RAFT[22] and initiators and initiators for continuous activator regeneration (ICAR) ATRP were used,[38] since both methods use radical initiators to drive the reaction forward. The results of this study indicated that the differences in the thermally initiated RDRP mechanisms are not significant at lower polymer chain lengths or DP, but larger differences in control are observed at high DP. A degradable crosslinker disulfide diacrylate or 2,2'-dithiodiethanol diacrylate (DSDA) was used to evaluate molecular properties of the network in addition to the bulk material characteristics of the networks synthesized by the relevant techniques.

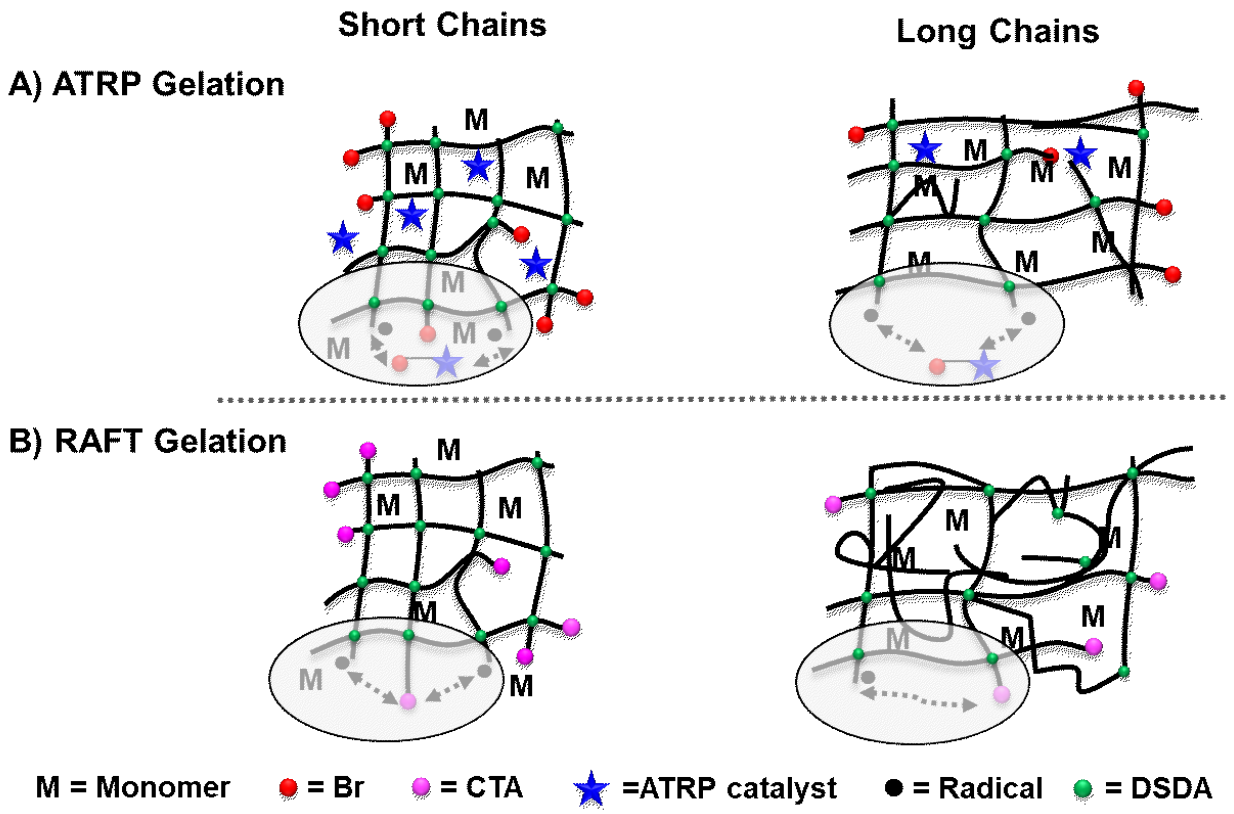

Figure 1. The hypothesized difference between ATRP and RAFT polymerizations for synthesizing networks during the sol and gelation phases and is dependent on chain length. A) The ATRP catalyst continues to mediate a controlled polymerization for short and long chain lengths. The Br chain end is transferred from the chain to the catalyst and a few monomers units add per cycle. B) In RAFT, the two chain ends must come into contact with each other, which is not feasible inside a long chain network in which the concentration of RAFT agent is low and therefore the polymerization is less controlled

Experimental Section

Materials: 2-Hydroxyethyl acrylate (HEA, 99%, TCI America) was purified using a basic alumina column (Ajax Chemical, AR) to remove inhibitors prior to use. *N*-Ethyl-*N*′-(3-dimethylaminopropyl)carbodiimide (EDC), copper(II) bromide ($CuBr_2$, 99%), 4-dimethylaminopyridine (DMAP), 1,4-dithiothreitol (DTT, >97%), and methyl 2-bromopropionate (MBP, 98%), acryloyl chloride (97%), triethylamine (TEA, ≥99%), bis(2-

hydroxyethyl) disulfide (BHEDS), were all purchased from Sigma-Aldrich and used as received. Tris(2-pyridylmethyl)amine (TPMA) was obtained from Koei Chemical and used as received. Deuterated dimethyl sulfoxide (DMSO-d6, 99.8%) was purchased from Cambridge Isotope Laboratories and used as received. 2,2'-Azobis (2-methylpropionitrile) (AIBN) was purchased from Sigma-Aldrich and recrystalized in ethanol. Dichloromethane (DCM), dimethylformamide (DMF), methanol (MeOH), and tetrahydrofuran (THF) were purchased from Fischer Scientific and used as received.

Synthesis of 2-(dodecylthiocarbonothioylthio)propionic acid or 2-(propionic acid)yldodecyl trithiocarbonate (PADTC)

PADTC was synthesized as indicated in the literature.[39]

Synthesis of the Disulfide Diacrylate (DSDA) or 2,2'-dithiodiethanol diacrylate

The synthesis of DSDA is detailed in the supporting information (**Scheme S1**, **Figure S1**).

Synthesis and Characterization of the ATRP Linear Polymer Models

The synthesis of the ATRP linear polymer models (**Scheme S2**, **Table S1**) and characterization (**Table S3**) is detailed in the supporting information.

General Procedure for Synthesis of the ATRP Networks

HEA, DSDA, $CuBr_2$/TPMA (from a stock solution $CuBr_2$ 10 mg/mL in DMF and TPMA 40 mg/mL in DMF), AIBN, and DMF were added. While stirring, the solution was sparged with nitrogen gas for 30 min in a glass vial (8 mL volume capacity) capped with a rubber septum. Under positive nitrogen pressure, the MBP (from a stock solution 50 mg/mL in DMF) was added to the pre-gel solution. A t=0 h ^{1}H NMR sample was taken from the pre-gel solution. The sealed vial placed in an oil bath at 65°C for 24 h to perform ICAR ATRP. The reaction was stopped by exposure to oxygen and cooling. The vinyl bond conversion was estimated by taking a piece of the as synthesized network and extraction of unreacted monomer and sol in DMSO-d_6. For all formation details, refer to **Table 1**.

Synthesis and Characterization of the RAFT Linear Polymer Models

The synthesis of the RAFT linear polymer models (**Scheme S3**, **Table S2**) and characterization (**Table S3**) is detailed in the supporting information.

General Procedure for the Synthesis of RAFT Networks

HEA, AIBN, DSDA, PADTC and DMF were mixed in a glass vial. A t=0 h ^{1}H NMR sample was taken from the pre-gel solution. The polymerization was carried out at 65°C for 24 h in a vial. For all formation details, refer to **Table 2**. The vinyl bond conversion was estimated by taking a piece of the as synthesized network and extraction of unreacted monomer and sol in DMSO-d_6.

Synthesis and Characterization of the Conventional FRP Networks

The synthesis of the conventional FRP networks (**Table S4**) and characterization (**Table S5**) is detailed in the supporting information.

Network Purification and Sol/Gel Fractions

All networks were washed 4× with methanol. Subsequently, the gels were dried by placing them in a desiccator, which was connected to the house vacuum for 7 days. To calculate the sol/gel fractions, the network samples (75-150 mg) were washed 4× with methanol and the wash solutions were collected and dried in order to calculate the sol/gel fractions.

$$Sol_{fraction} + Gel_{fraction} = 1 \qquad (1)$$

Swelling Experiments

The network samples (75-150 mg) were weighted and immersed in excess solvent (DMF) at room temperature (22°C). After 48 h, the samples were weighed. The swelling ratio was calculated as:

$$\text{Swelling ratio} = \frac{W_S - W_D}{W_D} \qquad (2)$$

where W_S and W_D are the weights of the swollen and dry gels respectively.

Network Degradation by Reducing the Disulfide Crosslinker

The disulfide crosslinker was cleaved to thiols using DTT, and the resulting soluble fractions were analyzed by SEC. Each of the FRP (**Table S5**), ATRP, and RAFT networks (20 mg) were immersed in a vial containing a 2 mL solution of DTT (25 mg/mL) in DMF. Each vial was sealed and sparged with nitrogen gas for 15 min, then heated at 65 °C for 24 h. The solutions obtained from the degradation procedure were analyzed by SEC.

Instrumentation

Size Exclusion Chromatography (SEC) was used for characterization of synthesized polymer with DMF as the eluent. DMF SEC analysis with different polymer samples was conducted with

a Waters 515 pump and Wyatt Optilab differential refractometer using poly(styrene sulfonate) columns (Styrogel 10^5, 10^3, and 10^2 Å) in 50 mM LiBr DMF solution as an eluent at 50 °C and at a flow rate of 1 mL min^{-1} . Linear poly(methyl methacrylate) (PMMA) standards were used for SEC calibration with SEC results analyzed in WinGPC 7.0 software from PSS for the DMF SEC.

Nuclear Magnetic Resonance (^{1}H NMR) was carried out with Bruker Ultrashield 500 MHz operating at 500 MHz or a Bruker 400 MHz NMR spectrometer for ^{1}H using DMSO-d_6 as the solvent.

Dynamic Mechanical Analysis- Mechanical properties of the networks were assessed using an Anton Paar MCR-302 Rheometer fitted with a parallel plate tool. Disk shaped gel samples with a thickness of 1-2 mm and diameter D = 8-25 mm were subjected to periodic torsional shearing between two parallel plates under a constant normal load of 2 N in the linear viscoelastic response region. The temperature ramps were carried out at a constant ramp of 2°C/min with a constant applied shear strain of 0.1% (γ) and a frequency (ω) of 10 rad/s.

Results and Discussion

Scheme 1. Mechanistic details of ICAR ATRP and RAFT (a) Schematic representation of ATRP mechanism (b) Main equilibrium step of RAFT mechanism.

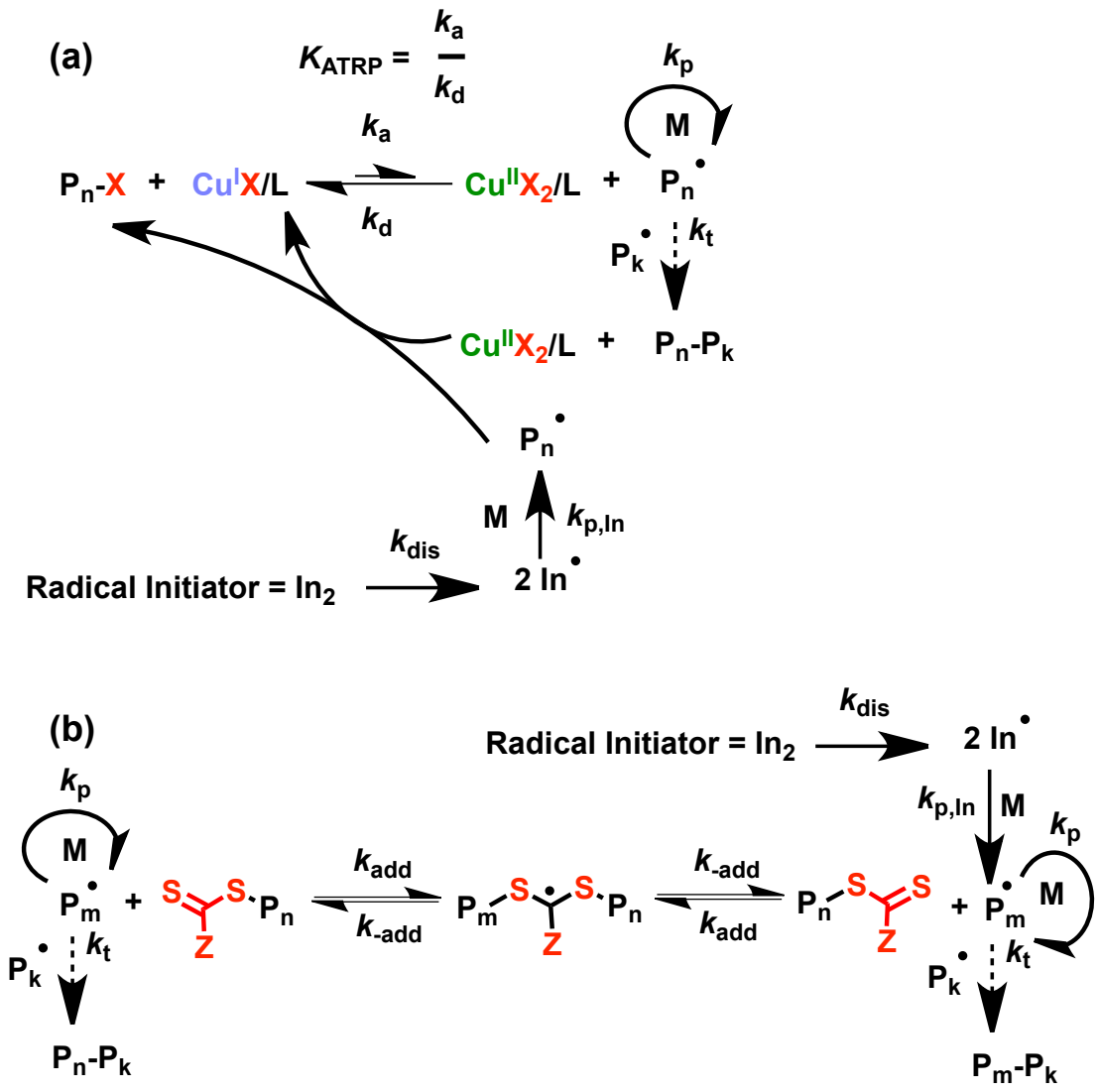

To compare the ATRP and RAFT networks, the specific ATRP and RAFT procedures were chosen to be as similar as possible. Therefore, thermally initiated RAFT polymerization and ICAR ATRP were used to compare the impact of these RDRP methods on the network properties. The same thermal initiator (AIBN) was used to generate radicals and drive polymerization to minimize the potential differences between the systems (**Scheme 1**). All polymers were synthesized at 65 °C for 24h. In RAFT polymerization, the initiating radicals react with the monomers and the CTAs.[21,22] ICAR ATRP is based on a reverse ATRP method when initiating radicals react with monomers and also reduce a deactivator $Cu^{II}Br_2$/L to form an activator $Cu^{I}Br$/L. The polymerization begins with only the deactivator $Cu^{II}Br_2$/L present in low (ppm) amounts,[38,40] with the radicals from the initiator generating the required $Cu^{I}Br$/L activator. Although both techniques are mechanistically

different, they are kinetically similar. In both cases, the rate of polymerization is ideally determined by the decomposition rate of the radical initiator. Importantly, the same fundamental differences in the exchange process between active and dormant species, discussed previously, remain. ICAR ATRP relies on a small molecule catalyst to transfer the atom (halogen) between the chain ends. RAFT polymerization relies on a transfer between polymer chain ends.

Scheme 2. A representation of the polymerization of (a) ATRP and (b) RAFT networks.

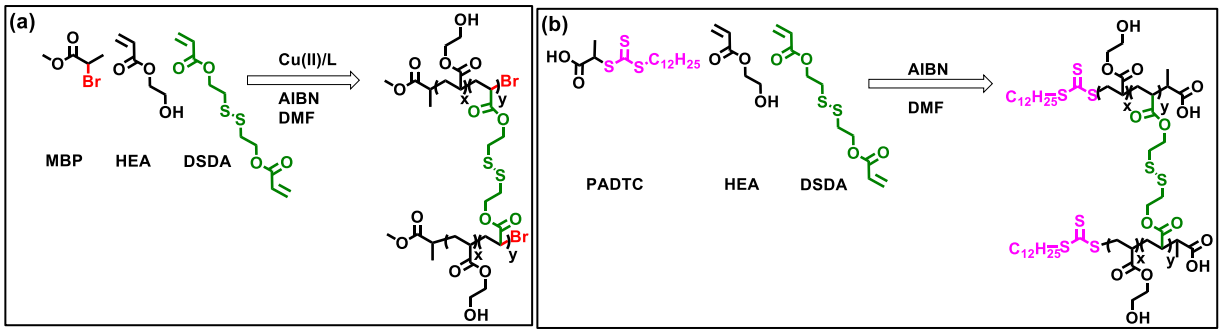

The networks were synthesized based on linear polymer models (**Scheme S2, Table S1, Scheme S3, Table S2, Table S3)** using 2-hydroxethyl acrylate (HEA) as the monomer and 2,2'-dithiodiethanol diacrylate (DSDA) as the crosslinker (**Scheme 2**). This crosslinker, containing a disulfide functional group, was used because it can be cleaved by a reduction reaction into two thiols. This approach was reported in order to study intermolecular branching and intramolecular cycling in RAFT networks.[41,42] In this study, cleaving the disulfide crosslinkers yielded soluble polymer chains for structural characterization by size exclusion chromatography (SEC). In total, twelve samples (ATRP, RAFT, and FRP) were prepared with a constant concentration of monomer (HEA), and the concentrations of the other materials being varied. The target DP of primary polymer chains (**Table 1**, **Table 2**), that is, the molar ratio of HEA to chain end (ATRP initiator or RAFT CTA) was DP 100, 200 and 500 and was used to compare the outcome of the polymerization while maintaining consistent compositions for both methods. The network mesh size was varied by the ratio of molar concentration of monomer and crosslinker. In addition, a series of FRP gels were prepared as reference materials, without ATRP initiators, copper/ligand complexes, or CTAs (Supporting information: General Procedure for the Synthesis of Conventional Free Radical Polymer (FRP) Networks, **Table S4**).

All networks were prepared in triplicate and the reactions were carried out at 65 °C for 24 h for consistency. After removal from the heat, the conversion of vinyl bonds was estimated by ^{1}H NMR. Subsequently, the networks were washed in excess methanol to remove unreacted monomer, sol, and solvent. After drying to remove any remaining methanol, the networks were characterized.

Table 1. The materials used for the synthesis of the four ATRP networks with the molar concentrations (M) specified.

Network Molar equiv.[1]	**[HEA][2]**	**[DSDA]**	**[MBP]**	**[$CuBr_2$][3]**	**[TPMA]**	**[AIBN]**
A100/5/1	4.35	2.2×10^{-1}	4.4×10^{-2}	8.7×10^{-4}	3.5×10^{-3}	8.7×10^{-3}
A200/5/1	4.35	1.1×10^{-1}	2.2×10^{-2}	4.4×10^{-4}	1.7×10^{-3}	4.4×10^{-3}
A500/5/1	4.35	4.4×10^{-2}	8.7×10^{-3}	1.7×10^{-4}	7.0×10^{-4}	1.7×10^{-3}
A500/3/1	4.35	2.6×10^{-2}	8.7×10^{-3}	1.7×10^{-4}	7.0×10^{-4}	1.7×10^{-3}

1) The molar equivalents are monomer/crosslinker/chain end (HEA/DSDA/MBP). 2) Solvent = DMF; Volume of the Solvent = Volume of the monomer. 3) In parts per million (ppm) relative to monomer (HEA), this would be: 200 ppm (A100/5/1), 100 ppm (A200/5/1), and 40 ppm (A500/5/1 and A500/3/1).

Table 2. The materials used for the synthesis of the four RAFT networks with the molar concentrations (M) specified.

Network Molar equiv.[1]	**[HEA][2]**	**[DSDA]**	**[PADTC]**	**[AIBN]**
R100/5/1	4.35	2.2×10^{-1}	4.4×10^{-2}	8.7×10^{-3}
R200/5/1	4.35	1.1×10^{-1}	2.2×10^{-2}	4.4×10^{-3}

R500/5/1	4.35	4.4×10^{-2}	8.7×10^{-3}	1.7×10^{-3}
R500/3/1	4.35	2.6×10^{-2}	8.7×10^{-3}	1.7×10^{-3}

1) The molar equivalents are HEA/DSDA/CTA. 2) Solvent = DMF; Volume of Solvent = Volume of monomer.

Molecular Characterization and Network Degradation

The conversion of monomer and crosslinker was determined from the decrease of vinyl proton signal in ^{1}H NMR. In living-like polymers, conversion is a critical parameter determining network formation and properties. Conversion, coupled with initial monomer, crosslinker, and initiator/CTA loading provides an average molecular weight between crosslinks (M_X) and network primary segment length (monomer units or molecular weight per chain). For example, in the A100/5/1 sample, if the polymerization reached full conversion, this would give an average of 17 HEA units between DSDA crosslinker, with primary chains of 100 units, based on the concept that average chain length between crosslinks M_x/M_{HEA} is given by:

$$M_x/M_{HEA} = \frac{[HEA]/[PADTC\ or\ MBP]}{1+[DSDA]/[PADTC\ or\ MBP]} \qquad (3)$$

where M_{HEA} is the molecular weight of the monomer HEA. The conversion is also necessary to calculate the theoretical molecular weight per chain ($M_{n,theo}$) for comparison to the degraded network $M_{n,app}$ determined by SEC. The RAFT and FRP networks reached greater than 95% conversion in all samples (**Error! Reference source not found.Table S5**). The ATRP networks reached lower conversion than the RAFT networks after 24 h of polymerization. Similar conversion trends have been reported in the literature.[26,36,43] The lower conversion in ATRP is likely because at the beginning of an ICAR ATRP reaction, there is an induction period during which $Cu^{II}Br_2$/L is reduced to Cu^{I}Br/L. In addition, catalyzed radical termination induced by Cu^{I} complexes in acrylate polymerization may accelerate termination and decrease polymerization rate.[44,45]

Although the ^{1}H NMR results only show the conversion of monomer to polymer in the system, the sol and gel fractions provide a better picture of the overall network formation. The sol refers to soluble, high molecular weight fractions that form during the gelation polymerization but did not connect to the infinite network. These fractions were removed by dialysis in a compatible solvent of methanol. The remaining insoluble materials form the gel fraction, with the sol and gel fractions determined according to eq. 1. The gel fraction was in all cases higher for the RAFT networks than for the ATRP networks (**Error! Reference source not found.Table 3**).

To determine the impact of the ATRP and RAFT mechanisms on the network segment homogeneity, the disulfide bonds in the crosslinker, DSDA, were cleaved, which allowed for soluble network segments to be analyzed by SEC. The disulfide crosslinker was cleaved to thiols using dithiothreitol (DTT), (**Figure 2Error! Reference source not found.**) and the resulting soluble fractions were analyzed by SEC (**Error! Reference source not found.**

Table *3*, **Table S5**). Each of the FRP, ATRP, and RAFT networks were immersed in a vial containing a solution of DTT and heated overnight. The solutions obtained from the degradation procedures were analyzed by SEC to determine the network segment length (ratio of HEA to chain end, either CTA or ATRP initiator), and molar mass dispersity. Whereas the ATRP and RAFT network samples completely degraded at the macroscopic level, the FRP gels were still present. Therefore, the SEC analysis from the FRP networks was performed on the solution present in the vial, but did not represent the network as a whole. This further supports the RDRP processes giving a more uniform network structure than the FRP process.

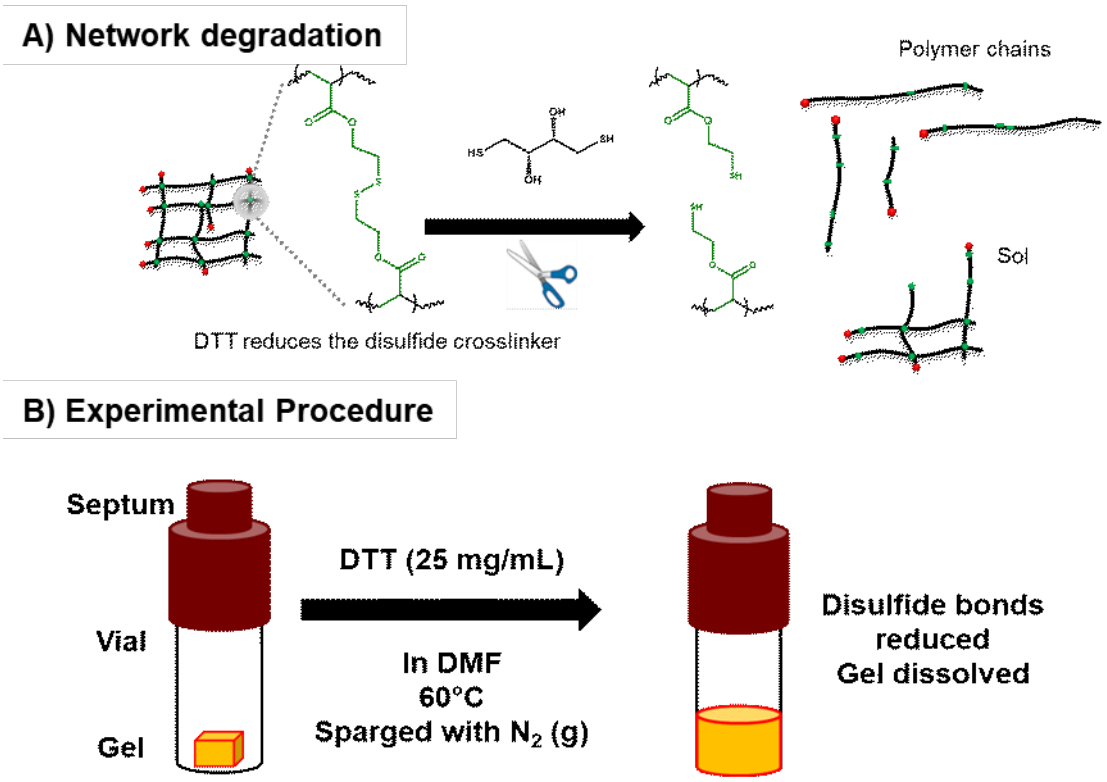

Figure 2. A) An illustration of the networks connected using the disulfide (DSDA) crosslinker and then degraded to release network segments (primary chains). B) Degradation in experimental view. The network (yellow cube) was placed in a vial containing DTT and DMF, then sealed, degassed, and heated. The solution obtained is shown in yellow (the color of the RAFT CTA) to indicate the degradation created soluble fractions.

Table 3. The structural data for networks formed by ATRP (A) and RAFT (R): conversion of vinyl bonds, gel fraction, the expected M_n of primary chains, the SEC M_n and dispersity after degradation of the networks. The samples are identified by the initial molar equivalents of monomer, crosslinker, and ATRP initiator/ CTA.

Sample	Conv. Vinyl Bonds (%)[1,2]	Gel Fraction[3]	$M_{n,theo}$[4]	$M_{n,app}$[5]	Đ[6]
A100/5/1	78 ± 9	0.87 ± 0.07	9.25×10^3	1.43×10^4	1.33 ± 0.04

R100/5/1	>95	0.95 ± 0.03	1.12×10^4	1.88×10^4	1.37 ± 0.05
A200/5/1	86 ± 4	0.87 ± 0.07	2.00×10^4	3.71×10^4	1.61 ± 0.09
R200/5/1	>95	0.90 ± 0.06	2.30×10^4	3.75×10^4	1.66 ± 0.05
A500/5/1	88 ± 3	0.8 ± 0.1	5.13×10^4	8.91×10^4	2.3 ± 0.2
R500/5/1	>95	0.90 ± 0.02	5.26×10^4	1.18×10^5	3.3 ± 0.6
A500/3/1	67 ± 12	0.83 ± 0.05	3.94×10^4	8.92×10^4	1.7 ± 0.2
R500/3/1	>95	0.88 ± 0.01	5.80×10^4	1.20×10^5	1.94 ± 0.02

The values reported are averages (n=3) and uncertainty (standard deviation). 1) The conversion of vinyl bonds was determined by ^{1}H NMR after 24 h. 2) In cases where the conversion is greater than 95%, >95 is reported due to the limited accuracy of the NMR. 3) Eq. 1: $Sol_{fraction} + Gel_{fraction} = 1$. 4) The $M_{n,theo}$ was calculated using the conversion determined by ^{1}H NMR. 5) The $M_{n,app}$ is the M_n observed by SEC (DMF). 6) The Đ observed by SEC (DMF).

The SEC results revealed the negligible differences between the two RDRP methods at lower primary chain lengths (DP = 100 and 200) but indicate some differences in molecular weight and dispersity at higher chain lengths (DP = 500) (

Table *3*). In all cases, the FRP soluble fractions yielded Đ ~2 (**Table S5**). However, it was not possible to fully degrade the networks under the same conditions as ATRP and RAFT, which confirms the increased structurally heterogeneity in FRP systems. In contrast, the Đ observed for the A100/5/1 and R100/5/1 were less than 1.4, comparable to a linear polymer model (**Table S3**), and the difference in average values was not statistically different. This showed that the polymerization remained controlled throughout the entire gelation process. Therefore, at the lower target DP = 100 and 200, the ATRP and RAFT processes formed linear polymers and the networks with similar structural control. Thus, the RAFT degenerative transfer process at this concentration

of CTA and primary chain length retains control despite the increase in viscosity during gelation and the need for the bimolecular exchange. The control in RAFT for these systems might also be attributed to the sol present. After the gel point in which the pre-gel solution transitions from a viscous liquid to a swollen network, there is still sol present inside the network. The sol could continue to diffuse within the network and the CTAs attached to the sol may facilitate degenerative chain transfer.

However, when the network chain length was increased to DP 500, both RDRP networks lost control compared to the linear models (**Table S3**), and the RAFT networks lost significantly more control than the ATRP networks. For example, for the A500/5/1 Đ was 2.3 ± 0.2, compared to the RAFT value of Đ 3.3 ± 0.6. For higher DP systems, where the RAFT agent is present in a much lower concentration, the degenerative transfer mechanism is hampered. This is not as significant in an ATRP system because the $Cu^{II}Br_2$/L is a small molecule and can better diffuse inside the network. In contrast, the RAFT agents are covalently attached to the network and this will limit diffusion and encounter with other chain ends. The ATRP network lost some control in the DP=500 systems due to the decreased concentration of $Cu^{II}Br_2$/L deactivator complex in ATRP, from 200 to 100 and eventually to 40 ppm vs. monomer (**Table 1**). It is noteworthy that the increase in dispersity was smaller for the high ratio of monomer to crosslinker A500/3/1 and R500/3/1. This suggests that the loss of control or decrease in exchange efficiency is not only related to chain length and concentration of the RAFT agent and $Cu^{II}Br_2$/L , but also to concentration of crosslinker, i.e., crosslinking density and a network mesh size. This is most likely due to the system with lower crosslink density having improved mobility and diffusion.

Network Characterization: Swelling Ratios

Swelling ratios are used to determine the solvent adsorption capacity of a network and can provide indirect information about the network structure and homogeneity. The experiments were performed by immersing the materials in excess DMF solvent for 48h. The swelling ratios was calculated according to eq. 2 (**Figure 3**). The degree of swelling increased as the ratio of monomer to crosslink increased in all cases. As the molar equivalents of HEA to DSDA increased, the M_x increased, and consequently the amount of solvent that can fill the network voids increased.

For every network iteration, the FRP networks had a significantly lower degree of swelling than the RDRP networks, consistent with literature reports.[1,25,35,37] This is due to the dense microclusters that form during the FRP gelation process and which limit swelling capacity. When comparing ATRP and RAFT networks, the average values and uncertainty were nearly identical for the A100/5/1 and R100/5/1 samples. As the network segment DP increased (and the concentration of crosslink point decreased), the average swelling of the ATRP and RAFT networks consistently increased. The greatest difference in results between ATRP and RAFT was for the 500/3/1 networks. The systems with chain lengths of DP=500 had the most significant difference in dispersity between ATRP and RAFT, with RAFT giving the higher dispersity. Also, the ATRP networks typically reached lower conversion than the RAFT materials, suggesting fewer monomeric and divinyl bonds are incorporated. Since a more homogeneous network is typically correlated with higher swelling, the somewhat enhanced swelling of the chain length 500 ATRP networks compared to their RAFT counterparts was consistent with the differences in vinyl bond conversion and dispersity observed (

Table *3*). However, it is important to emphasize that the key differences in swelling ratio are between the FRP and RDRP networks, and with relatively small differences between the RDRP ones.

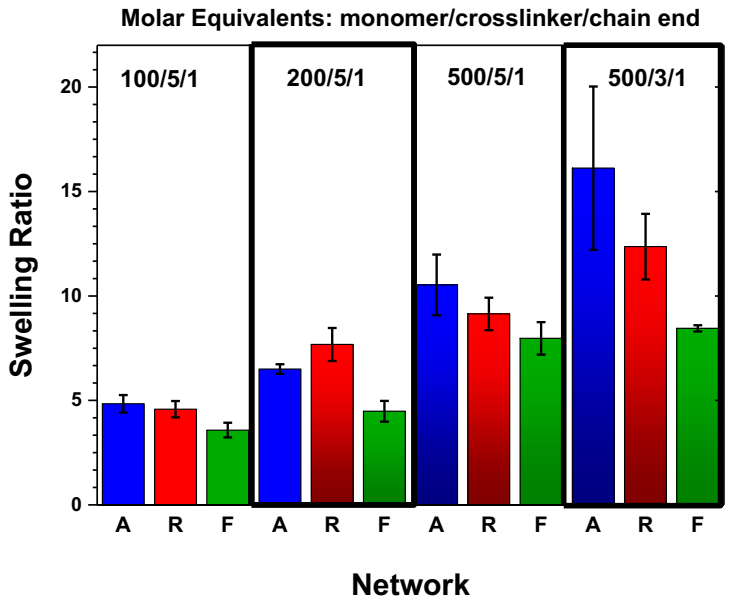

Figure 3. The average swelling ratios of networks after immersion in DMF calculated according to eq. 2. For clarity in the figure, the polymer synthesis method has been abbreviated by the first letter: ATRP (A, blue); RAFT (R, red); FRP (F, green). The uncertainty (black bars) were the standard deviation (n=6). The swollen networks are grouped according to the molar equivalents of monomer/crosslinker/chain end, although there is no chain end in the case of the FRP networks.

Rheological Analysis

To gain insights into the network structure, oscillatory shear rheology tests were performed on the dry polymer networks. As noted earlier, it is challenging to analyze the internal structure of gels and networks. Although rheological tests characterize how the entire material behaves in response to stress or strain, the data obtained can provide indirect information about the internal network structure. Polymer networks are known to exhibit both elastic (solid-like) and viscous (liquid-like) behavior, which were recorded as the storage (G′), and loss (G″) moduli, respectively. Important for understanding the structure of the ATRP, RAFT and FRP networks was their ratio (G″/G′), which is the dampening factor (tan (δ)). Tan(δ) is a measure of energy dissipation and, therefore, can be used to determine phase transitions, including the glass transition temperature (T_g). In networks, the T_g occurs over a temperature range.

The networks were analyzed by oscillatory shear frequency sweeps at room temperature as an indirect method of assessing molecular weight between crosslink points (**Figure 4**, **Figure S2**). Note that typical errors in rheological experiments are in the order of 10%, when measured on shear thinning fluids.[46] The material modulus is inversely related to the molecular weight between crosslinks in the polymer chains. Using the affine model of networks, the shear modulus and the M_x is commonly related by the following equation:

$$G = \frac{\rho RT}{M_x} \qquad (4)$$

where G is the shear modulus, ρ is the density, R is the gas constant, T is the temperature, and M_x is the molecular weight between crosslink points. That is, lower the molecular weight between crosslinks, the higher the modulus value and vice versa. The networks were subjected to different oscillation frequencies from 0.1 to 100 rad/s. The lowest frequency (0.1 rad/s) is an indication behavior at long timescales or "rest behavior," whereas the highest frequency (100 rad/s) is an indication of behavior at short timescales. Therefore, comparing the G′ (Pa) values provides a relative indication of the average M_x through the entire material.

The measured G′ at low frequency (0.1 rad/s) should decrease with larger M_x values, that is, A/R100/5/1 > A/R200/5/1 > A/R500/5/1 > A/R500/3/1. This is the trend that was observed for both ATRP and RAFT networks, but with some significant differences. For instance, the values of G′ varied substantially more for the ATRP networks as compared to the RAFT networks. This would suggest structural differences between the networks that were not captured by the SEC traces. Ideally, two materials with the same composition should have similar M_x and therefore G' values at low frequency. For example, the higher R500/5/1 G′ at 0.1 rad/s compared to the A500/5/1 could result from the lower monomer conversion typical of the ATRP networks. In addition, the SEC results show that the R500/5/1 and R500/3/1 degraded network samples had a consistently higher Đ than the ATRP counterparts, suggesting that there is more heterogeneity of crosslink junctions throughout the RAFT networks. Another contributing factor is the greater sol fraction present in the ATRP networks compared to the RAFT networks, which could have a plasticizing effect on the network.

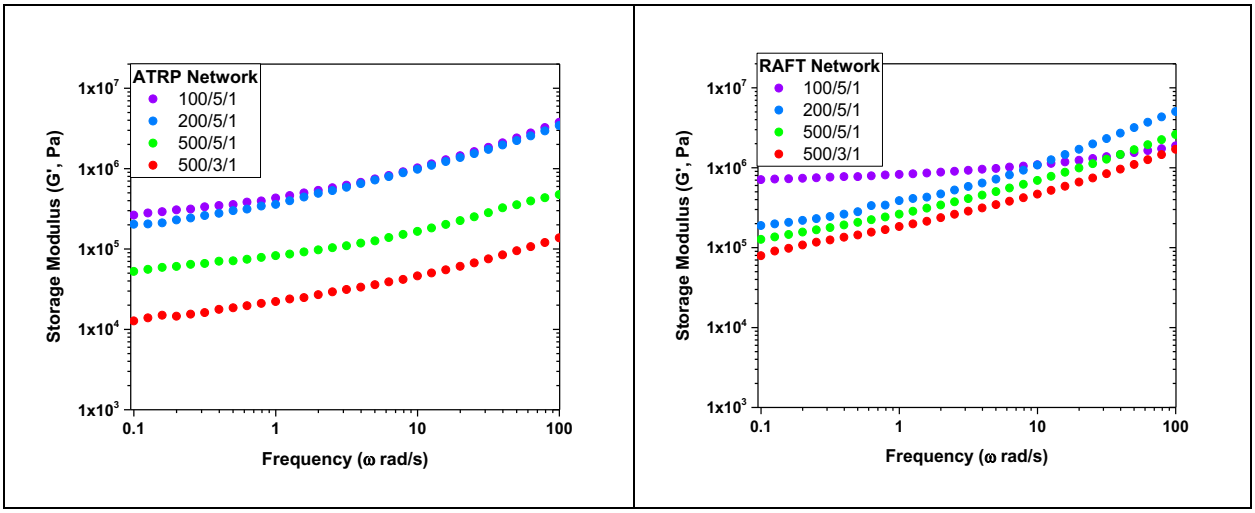

Figure 4. The frequency sweeps for the network samples that show the storage (G′) ATRP (left) and RAFT (right). The legend indicates the molar ratios of the monomer/crosslinker/chain end. Performed at room temperature (25°C); γ = 0.1%; applied normal force 2 N. The networks were analyzed after purification and in the dry state.

Additionally, the networks' behavior was studied over a temperature range between the glassy plateau (vitrified state below the glass transition temperature (T_g)) and the rubbery plateau (rubbery state above the T_g) from approximately -30 ºC to 60 ºC for these PHEA based networks (**Figure 5**, **Figure 6**, **Figure S3**, and **Figure S4**). It was observed that the G′ values in the rubbery plateau region (60 ºC) followed the anticipated trend, A/R100/5/1 > A/R200/5/1 > A/R500/5/1 > A/R500/3/1. These values were in agreement with the ones observed in the frequency sweeps.

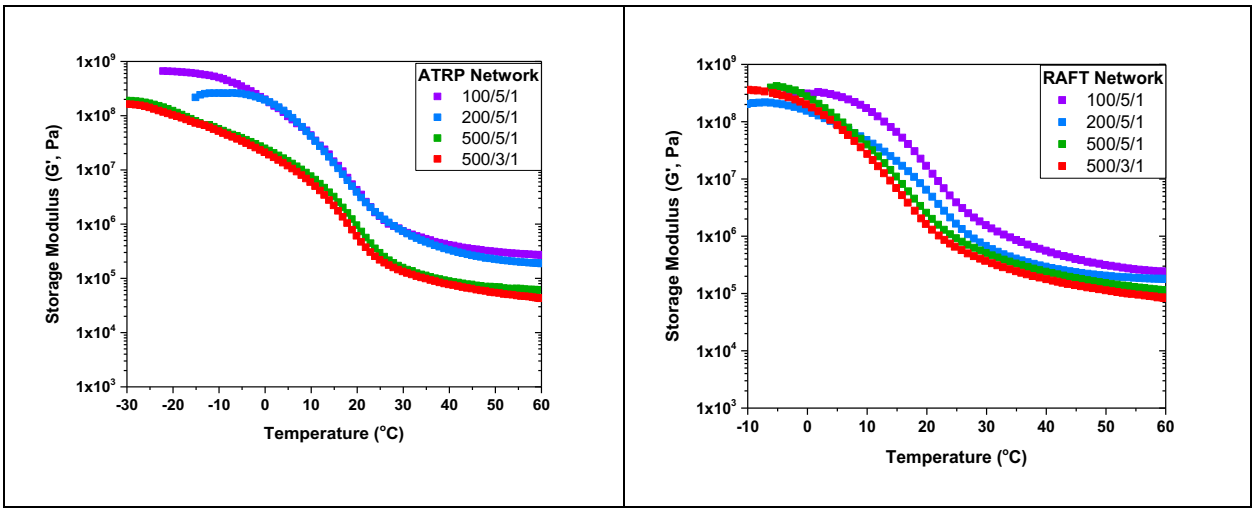

Figure 5. The temperature for the network samples that show the storage modulus (G′) and ATRP (left) and RAFT (right). The legend indicates the molar ratios of the monomer/crosslinker/chain end. Temperature Sweeps: heating rate = 2°C/min; γ = 0.1%; ω = 10 rad/s; applied normal force 2 N. The networks were analyzed after purification and in the dry state.

The tan (δ) profiles vs temperature was also important to understand any differences or similarities between the two RDRP methods (**Figure 6**, **Figure S4, Figure S5**). The tan (δ) profile can be used to observe transition areas in the viscoelastic material response. Therefore, the tan (δ) can be used to determine the T_g, which is the transition between the glassy or immobilized state and rubbery state where chains can move and relax. The peak of the tan (δ) curve can be taken as the T_g value.[47,48] As expected of a PHEA network, the T_g values were between 17-25 ºC. It was observed that the maximum tan (δ) value decreased slightly as the M_x increased. All of the profiles were similar, with the exception of the A500/5/1 and A500/3/1, which showed a shoulder below the maximum tan (δ). This is attributed to sol still present in the ATRP networks. As was previously observed, the sol fraction was higher for the ATRP networks than the RAFT ones (

Table *3*Error! Reference source not found.). Indeed, repeated washes on these networks decreased the magnitude of this peak. (**Figure S5**) The sol fractions have a plasticizing effect on the network, which would explain some of the substantially low G′ values in the ATRP networks compared to the RAFT networks.

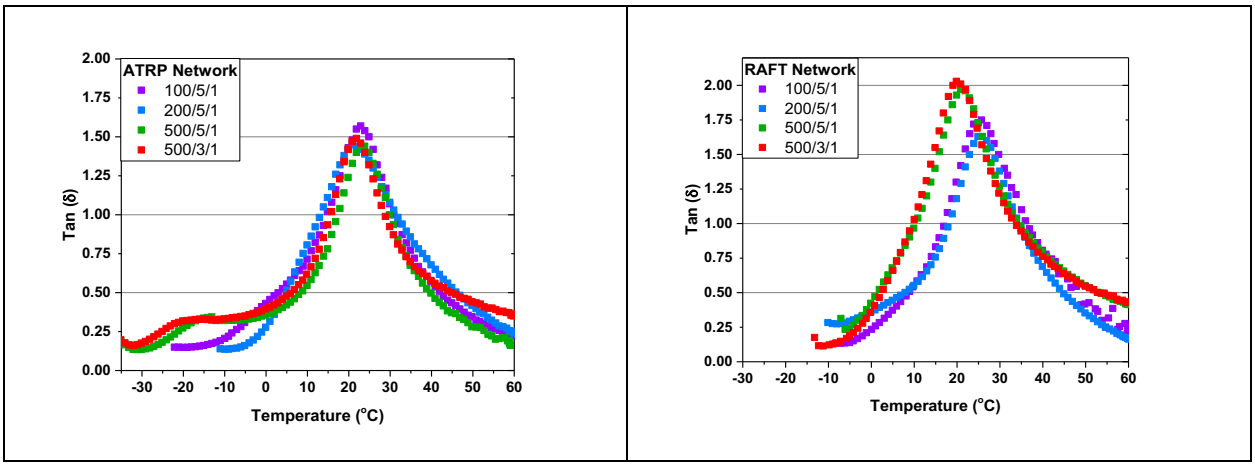

Figure 6. The temperature for the network samples that show the tan (δ) profile vs temperature and ATRP (left) and RAFT (right). The legend indicates the molar ratios of the monomer/crosslinker/chain end. Temperature Sweeps: heating rate = 2 °C/min; γ = 0.1%; ω = 10 rad/s; applied normal force 2 N. The networks were analyzed after purification and in the dry state. The ATRP 500/5/1 and 500/3/1 profile are the results after a further purification step, for a total of 8× MeOH washes.

Conclusions

Although there have been reports on the differences between gel structures prepared by FRP and RDRP, there has not been systematic study of the differences between gels formed by ATRP and RAFT. Therefore, ATRP and RAFT networks were synthesized using thermally initiated polymerization methods with similar kinetics. By utilizing cleavable crosslinkers, it was possible to degrade the networks and analyze the primary chains by SEC. This demonstrated that there was little difference between the gelation processes and networks with primary chain lengths of DP=100 and 200. However, for higher DP of 500, the ATRP networks had lower Đ than the RAFT counterparts. The rheological analysis and swelling experiments showed that the ATRP and RAFT networks had similar physical properties, T_g and swelling capacity. However, changing the chain length/M_x had a more pronounced effect on the ATRP network modulus than the RAFT. Therefore, it can be concluded that the two polymerization methods produce comparable networks at low chain length, but ATRP maintains better control at higher primary chain length, although RAFT reaches higher conversions and gel fractions. It is important to understand the differences in structure and properties of all these materials, not only for the pursuit of scientific knowledge, but also for practical applications. It is hoped that these results will enable future research to select polymerization methods tailored to the desired material properties.

ASSOCIATED CONTENT

Supporting Information Additional experimental details and procedures, characterization data of FRP synthesized networks, supplementary rheological characterization.

AUTHOR INFORMATION

Corresponding Author

Corresponding authors: Krzysztof Matyjaszewski: matyjaszewski@cmu.edu, and Dominik Konkolewicz: d.konkolewicz@miamiOH.edu

Author Contributions

The manuscript was written through contributions of all authors. All authors have given approval to the final version of the manuscript. ‡Shiwanka V. Wanasinghe and Julia Cuthbert contributed equally.

ACKNOWLEDGMENT

The Matyjaszewski group gratefully acknowledges support from the Department of Energy (grant ER45998) for ATRP materials development. The Konkolewicz group gratefully acknowledges support from the National Science Foundation under Grant No. (DMR-1749730) for RAFT materials development. The Konkolewicz group would also like to acknowledge support from the Robert H. and Nancy J. Blayney Professorship for supporting equipment. The NMR facility at CMU was partially supported by NSF grants CHE-9808188, CHE-1039870 and CHE-1726525. 400 MHz NMR instrumentation at Miami University is supported through funding from the National Science Foundation under grant number (CHE- 1919850). The Matyjaszewski group also gratefully acknowledges Koei Chemical for providing the TPMA.

REFERENCES

(1) Gao, H.; Matyjaszewski, K. Synthesis of functional polymers with controlled architecture by CRP of monomers in the presence of cross-linkers: From stars to gels. *Progress in Polymer Science* **2009**, *34*, 317-350.

(2) Gao, H.; Min, K.; Matyjaszewski, K. Determination of Gel Point during Atom Transfer Radical Copolymerization with Cross-Linker. *Macromolecules* **2007**, *40*, 7763-7770.

(3) Di Lorenzo, F.; Seiffert, S. Nanostructural heterogeneity in polymer networks and gels. *Polymer Chemistry* **2015**, *6*, 5515-5528.

(4) Danielsen, S. P. O.; Beech, H. K.; Wang, S.; El-Zaatari, B. M.; Wang, X.; Sapir, L.; Ouchi, T.; Wang, Z.; Johnson, P. N.; Hu, Y.; Lundberg, D. J.; Stoychev, G.; Craig, S. L.; Johnson, J. A.; Kalow, J. A.; Olsen, B. D.; Rubinstein, M. Molecular Characterization of Polymer Networks. *Chemical Reviews* **2021**, *121*, 5042-5092.

(5) Gu, Y.; Zhao, J.; Johnson, J. A. A (Macro)Molecular-Level Understanding of Polymer Network Topology. *Trends in Chemistry* **2019**, *1*, 318-334.

(6) De Alwis Watuthanthrige, N.; Chakma, P.; Konkolewicz, D. Designing Dynamic Materials from Dynamic Bonds to Macromolecular Architecture. *Trends in Chemistry* **2021**, *3*, 231-247.

(7) De Keer, L.; Kilic, K. I.; Van Steenberge, P. H. M.; Daelemans, L.; Kodura, D.; Frisch, H.; De Clerck, K.; Reyniers, M.-F.; Barner-Kowollik, C.; Dauskardt, R. H.; D'hooge, D. R. Computational prediction of the molecular configuration of three-dimensional network polymers. *Nature Materials* **2021**.

(8) Richbourg, N. R.; Peppas, N. A. The swollen polymer network hypothesis: Quantitative models of hydrogel swelling, stiffness, and solute transport. *Progress in Polymer Science* **2020**, *105*, 101243.

(9) Carothers, W. H. Polymers and polyfunctionality. *Transactions of the Faraday Society* **1936**, *32*, 39-49.

(10) Flory, P. J. Constitution of Three-dimensional Polymers and the Theory of Gelation. *The Journal of Physical Chemistry* **1942**, *46*, 132-140.

(11) Stockmayer, W. H. Theory of Molecular Size Distribution and Gel Formation in Branched Polymers II. General Cross Linking. *The Journal of Chemical Physics* **1944**, *12*, 125-131.

(12) Flory, P. J.: *Principles of polymer chemistry*, 1953.

(13) De Keer, L.; Van Steenberge, P. H. M.; Reyniers, M.-F.; D'hooge, D. R. Going Beyond the Carothers, Flory and Stockmayer Equation by Including Cyclization Reactions and Mobility Constraints. *Polymers* **2021**, *13*, 2410.

(14) Gu, Y.; Zhao, J.; Johnson, J. A. Polymer Networks: From Plastics and Gels to Porous Frameworks. *Angewandte Chemie International Edition* **2020**, *59*, 5022-5049.

(15) Gu, Y.; Kawamoto, K.; Zhong, M.; Chen, M.; Hore, M. J. A.; Jordan, A. M.; Korley, L. T. J.; Olsen, B. D.; Johnson, J. A. Semibatch monomer addition as a general method to tune and enhance the mechanics of polymer networks via loop-defect control. *Proceedings of the National Academy of Sciences* **2017**, *114*, 4875.

(16) Huang, X.; Nakagawa, S.; Li, X.; Shibayama, M.; Yoshie, N. A Simple and Versatile Method for the Construction of Nearly Ideal Polymer Networks. *Angewandte Chemie* **2020**, *59*, 9646-9652.

(17) Nakagawa, S.; Yoshie, N. Synthesis of a Bottlebrush Polymer Gel with a Uniform and Controlled Network Structure. *ACS Macro Letters* **2021**, *10*, 186-191.

(18) Wang, J. S.; Matyjaszewski, K. Controlled Living Radical Polymerization - Atom-Transfer Radical Polymerization in the Presence of Transition-Metal Complexes. *Journal of the American Chemical Society* **1995**, *117*, 5614-5615.

(19) Matyjaszewski, K. Atom Transfer Radical Polymerization (ATRP): Current Status and Future Perspectives. *Macromolecules* **2012**, *45*, 4015-4039.

(20) Matyjaszewski, K. Advanced Materials by Atom Transfer Radical Polymerization. *Advanced Materials* **2018**, *30*, 1706441.

(21) Chiefari, J.; Chong, Y. K.; Ercole, F.; Krstina, J.; Jeffery, J.; Le, T. P. T.; Mayadunne, R. T. A.; Meijs, G. F.; Moad, C. L.; Moad, G.; Rizzardo, E.; Thang, S. H. Living Free-Radical Polymerization by Reversible Addition–Fragmentation Chain Transfer: The RAFT Process. *Macromolecules* **1998**, *31*, 5559-5562.

(22) Perrier, S. 50th Anniversary Perspective: RAFT Polymerization—A User Guide. *Macromolecules* **2017**, *50*, 7433-7447.

(23) Moad, G. RAFT (Reversible addition–fragmentation chain transfer) crosslinking (co)polymerization of multi-olefinic monomers to form polymer networks. *Polymer International* **2015**, *64*, 15-24.

(24) Ide, N.; Fukuda, T. Nitroxide-Controlled Free-Radical Copolymerization of Vinyl and Divinyl Monomers. Evaluation of Pendant-Vinyl Reactivity. *Macromolecules* **1997**, *30*, 4268-4271.

(25) Ide, N.; Fukuda, T. Nitroxide-Controlled Free-Radical Copolymerization of Vinyl and Divinyl Monomers. 2. Gelation. *Macromolecules* **1999**, *32*, 95-99.

(26) Yu, Q.; Xu, S.; Zhang, H.; Ding, Y.; Zhu, S. Comparison of reaction kinetics and gelation behaviors in atom transfer, reversible addition–fragmentation chain transfer and conventional free radical copolymerization of oligo(ethylene glycol) methyl ether methacrylate and oligo(ethylene glycol) dimethacrylate. *Polymer* **2009**, *50*, 3488-3494.

(27) Wang, R.; Luo, Y.; Li, B.-G.; Zhu, S. Modeling of Branching and Gelation in RAFT Copolymerization of Vinyl/Divinyl Systems. *Macromolecules* **2009**, *42*, 85-94.

(28) Joubert, F.; Cheong Phey Denn, P.; Guo, Y.; Pasparakis, G. Comparison of Thermoresponsive Hydrogels Synthesized by Conventional Free Radical and RAFT Polymerization. *Materials* **2019**, *12*, 2697.

(29) Whitfield, R.; Parkatzidis, K.; Rolland, M.; Truong, N. P.; Anastasaki, A. Tuning Dispersity by Photoinduced Atom Transfer Radical Polymerisation: Monomodal Distributions with ppm Copper Concentration. *Angewandte Chemie International Edition* **2019**, *58*, 13323-13328.

(30) Soeriyadi, A. H.; Boyer, C.; Nyström, F.; Zetterlund, P. B.; Whittaker, M. R. High-Order Multiblock Copolymers via Iterative Cu(0)-Mediated Radical Polymerizations (SET-LRP): Toward Biological Precision. *J Am Chem Soc* **2011**, *133*, 11128-11131.

(31) Carmean, R. N.; Becker, T. E.; Sims, M. B.; Sumerlin, B. S. Ultra-High Molecular Weights via Aqueous Reversible-Deactivation Radical Polymerization. *Chem* **2017**, *2*, 93-101.

(32) Gody, G.; Maschmeyer, T.; Zetterlund, P. B.; Perrier, S. Rapid and quantitative one-pot synthesis of sequence-controlled polymers by radical polymerization. *Nature Communications* **2013**, *4*, 2505.

(33) Whitfield, R.; Parkatzidis, K.; Truong, N. P.; Junkers, T.; Anastasaki, A. Tailoring Polymer Dispersity by RAFT Polymerization: A Versatile Approach. *Chem* **2020**, *6*, 1340-1352.

(34) Yoon, J. A.; Bencherif, S. A.; Aksak, B.; Kim, E. K.; Kowalewski, T.; Oh, J. K.; Matyjaszewski, K. Thermoresponsive Hydrogel Scaffolds with Tailored Hydrophilic Pores. *Chemistry – An Asian Journal* **2011**, *6*, 128-136.

(35) Yoon, J. A.; Gayathri, C.; Gil, R. R.; Kowalewski, T.; Matyjaszewski, K. Comparison of the Thermoresponsive Deswelling Kinetics of Poly(2-(2-methoxyethoxy)ethyl methacrylate) Hydrogels Prepared by ATRP and FRP. *Macromolecules* **2010**, *43*, 4791-4797.

(36) Norioka, C.; Kawamura, A.; Miyata, T. Mechanical and responsive properties of temperature-responsive gels prepared via atom transfer radical polymerization. *Polymer Chemistry* **2017**, *8*, 6050-6057.

(37) Liu, Q.; Zhang, P.; Qing, A.; Lan, Y.; Lu, M. Poly(N-isopropylacrylamide) hydrogels with improved shrinking kinetics by RAFT polymerization. *Polymer* **2006**, *47*, 2330-2336.

(38) Matyjaszewski, K.; Jakubowski, W.; Min, K.; Tang, W.; Huang, J.; Braunecker, W. A.; Tsarevsky, N. V. Diminishing catalyst concentration in atom transfer radical polymerization with reducing agents. *Proceedings of the National Academy of Sciences* **2006**, *103*, 15309.

(39) Craig, A. F.; Clark, E. E.; Sahu, I. D.; Zhang, R.; Frantz, N. D.; Al-Abdul-Wahid, M. S.; Dabney-Smith, C.; Konkolewicz, D.; Lorigan, G. A. Tuning the size of styrene-maleic acid copolymer-lipid nanoparticles (SMALPs) using RAFT polymerization for biophysical studies. *Biochimica et Biophysica Acta (BBA) - Biomembranes* **2016**, *1858*, 2931-2939.

(40) Krys, P.; Ribelli, T. G.; Matyjaszewski, K.; Gennaro, A. Relation between Overall Rate of ATRP and Rates of Activation of Dormant Species. *Macromolecules* **2016**, *49*, 2467-2476.

(41) Rosselgong, J.; Armes, S. P. Quantification of Intramolecular Cyclization in Branched Copolymers by 1H NMR Spectroscopy. *Macromolecules* **2012**, *45*, 2731-2737.

(42) Estupiñán, D.; Barner-Kowollik, C. Counting the Clicks in Fluorescent Polymer Networks. **2018**, *57*, 5925-5929.

(43) Gonçalves, M. A. D.; Pinto, V. D.; Costa, R. A. S.; Dias, R. C. S.; Hernándes-Ortiz, J. C.; Costa, M. R. P. F. N. Stimuli-Responsive Hydrogels Synthesis using Free Radical and RAFT Polymerization. *Macromolecular Symposia* **2013**, *333*, 41-54.

(44) Wang, Y.; Soerensen, N.; Zhong, M.; Schroeder, H.; Buback, M.; Matyjaszewski, K. Improving the "Livingness" of ATRP by Reducing Cu Catalyst Concentration. *Macromolecules* **2013**, *46*, 683-691.

(45) Ribelli, T. G.; Rahaman, S. M. W.; Matyjaszewski, K.; Poli, R.: Catalyzed Radical Termination (CRT) in the Metal-Mediated Polymerization of Acrylates: Experimental and Computational Studies. In *Reversible Deactivation Radical Polymerization: Mechanisms and Synthetic Methodologies*; ACS Symposium Series 1284; American Chemical Society, 2018; Vol. 1284; pp 135-159.

(46) Escudier, M. P.; Gouldson, I. W.; Pereira, A. S.; Pinho, F. T.; Poole, R. J. On the reproducibility of the rheology of shear-thinning liquids. *Journal of Non-Newtonian Fluid Mechanics* **2001**, *97*, 99-124.

(47) Nielsen, L. E.; Landel, R. F.: *Mechanical properties of polymers and composites*; 2nd ed.; M. Dekker: New York, 1994.

(48) Yong, A. X. H.; Sims, G. D.; Gnaniah, S. J. P.; Ogin, S. L.; Smith, P. A. Heating rate effects on thermal analysis measurement of Tg in composite materials. *Advanced Manufacturing: Polymer & Composites Science* **2017**, *3*, 43-51.

for Table of Contents use only

Are RAFT and ATRP Universally Interchangeable Polymerization Methods in Network Formation?

Julia Cuthbert, Shiwanka V. Wanasinghe, Krzysztof Matyjaszewski, Dominik Konkolewicz